IOPscience iopscience.iop.org

Home Search Collections Journals About Contact us My IOPscience

Rashbons: properties and their significance

This content has been downloaded from IOPscience. Please scroll down to see the full text.

2012 New J. Phys. 14 043041

(http://iopscience.iop.org/1367-2630/14/4/043041)

View the table of contents for this issue, or go to the journal homepage for more

Download details:

IP Address: 117.192.196.111
This content was downloaded on 29/03/2017 at 14:20

Please note that terms and conditions apply.

You may also be interested in:

Fermions in synthetic non-Abelian gauge potentials: rashbon condensates to novel Hamiltonians
Vijay B Shenoy and Jayantha P Vyasanakere

Degenerate quantum gases with spin–orbit coupling: a review
Hui Zhai

Comparing and contrasting nuclei and cold atomic gases
N T Zinner and A S Jensen

Fulde–Ferrell superfluidity in ultracold Fermi gases with Rashba spin–orbit coupling
Hui Hu and Xia-Ji Liu

Pair condensation in a dilute Bose gas with Rashba spin–orbit coupling
Rong Li and Lan Yin

Strongly correlated quantum fluids: ultracold quantum gases, quantum chromodynamic plasmas and holographic duality
Allan Adams, Lincoln D Carr, Thomas Schäfer et al.

Models of coherent exciton condensation
P B Littlewood, P R Eastham, J M J Keeling et al.

Fulde–Ferrell pairing instability in spin–orbit coupled Fermi gas
Lin Dong, Lei Jiang and Han Pu

Pseudogap and preformed pairs in the imbalanced Fermi gas in two dimensions
S N Klimin, J Tempere and J T Devreese

New Journal of Physics
The open-access journal for physics

Rashbons: properties and their significance

Jayantha P Vyasanakere and Vijay B Shenoy
Centre for Condensed Matter Theory, Department of Physics,
Indian Institute of Science, Bangalore 560 012, India
E-mail: jayantha@physics.iisc.ernet.in and shenoy@physics.iisc.ernet.in

New Journal of Physics **14** (2012) 043041 (14pp)
Received 28 December 2011
Published 27 April 2012
Online at http://www.njp.org/
doi:10.1088/1367-2630/14/4/043041

Abstract. In the presence of a synthetic non-Abelian gauge field that produces a Rashba-like spin–orbit interaction, a collection of weakly interacting fermions undergoes a crossover from a Bardeen–Cooper–Schrieffer (BCS) ground state to a Bose–Einstein condensate (BEC) ground state when the strength of the gauge field is increased (Vyasanakere *et al* 2011 *Phys. Rev.* B **84** 014512). The BEC that is obtained at large gauge coupling strengths is a condensate of tightly bound bosonic fermion pairs. The properties of these bosons are solely determined by the Rashba gauge field—hence called rashbons. In this paper, we conduct a systematic study of the properties of rashbons and their dispersion. This study reveals a new qualitative aspect of the problem of interacting fermions in non-Abelian gauge fields, i.e. that the rashbon state ceases to exist when the center-of-mass momentum of the fermions exceeds a critical value that is of the order of the gauge coupling strength. The study allows us to estimate the transition temperature of the rashbon BEC and suggests a route to enhance the exponentially small transition temperature of the system with a fixed weak attraction to the order of the Fermi temperature by tuning the strength of the non-Abelian gauge field. The nature of the rashbon dispersion, and in particular the absence of the rashbon states at large momenta, suggests a regime in parameter space where the normal state of the system will be a dynamical mixture of uncondensed rashbons and unpaired helical fermions. Such a state should show many novel features including pseudogap physics.

© IOP Publishing Ltd and Deutsche Physikalische Gesellschaft

Contents

1. Introduction

Cold atoms are a promising platform for quantum simulations. The controlled generation of synthetic gauge fields [1–3] has provided an impetus to the realization of novel phases in cold atomic systems. The recent generation of synthetic non-Abelian gauge fields in ^{87}Rb atoms [3] is a key step forward in this regard. While a uniform Abelian gauge field is merely equivalent to a Galilean transformation, a uniform non-Abelian gauge field nurtures interesting physics [3–5].

The clue that a uniform non-Abelian gauge field crucially influences the physics of interacting fermions came from a study of bound states of two spin-$\frac{1}{2}$ fermions in its presence [6]. The remarkable result found for spin-$\frac{1}{2}$ fermions in three spatial dimensions interacting via an s-wave contact interaction in the singlet channel is that high-symmetry non-Abelian gauge field configurations (GFCs) induce a two-body bound state for *any* scattering length, however small and negative. The physics behind this unusual role of the non-Abelian gauge field that produces a generalized Rashba spin–orbit interaction was explained by its effect on the infrared density of states of the noninteracting two-particle spectrum. The non-Abelian gauge field drastically enhances the infrared density of states, and this serves to 'amplify the attractive interactions'. A second remarkable feature demonstrated in [6] is that the wave function of the bound state that emerges has a triplet content and an associated spin-nematic structure similar to those found in liquid ^{3}He.

The above-mentioned study [6] motivated the study of interacting fermions at a *finite* density in the presence of a non-Abelian gauge field [7]. At a finite density ρ ($\sim k_{\mathrm{F}}^3$, k_{F} is the Fermi momentum), the physics of interacting fermions in a synthetic non-Abelian gauge field is determined by two dimensionless scales. The first scale is associated with the size of the interactions $-1/k_{\mathrm{F}}a_{\mathrm{s}}$, where a_{s} is the s-wave scattering length, and the second one, λ/k_{F}, is determined by the non-Abelian gauge coupling strength λ. For small negative scattering lengths ($-1/k_{\mathrm{F}}a_{\mathrm{s}} \gg 1$), the ground state in the absence of the gauge field is a BCS superfluid state with large overlapping pairs. The key result first demonstrated in [7] is that at a *fixed scattering length*, even if small and negative, the non-Abelian gauge field induces a crossover of the ground

state from the just discussed Bardeen–Cooper–Schrieffer (BCS) superfluid state to a new type of Bose–Einstein condensate (BEC) state. The BEC state that emerges is a condensate of a collection of bosons which are tightly bound pairs of fermions. Remarkably, at large gauge couplings $\lambda \gg k_F$, the nature of the bosons that make up the condensate is determined *solely by the gauge field* and is not influenced by the scattering length (as long as it is nonzero) or by the density of particles. In other words, the BEC state that is attained in the $\lambda \gg k_F$ regime at a fixed scattering length does not depend on the value of the scattering length, i.e. the BEC is a condensate of a novel bosonic paired state of fermions determined by the non-Abelian gauge field. These bosons were called 'rashbons' since their properties are determined solely by the generalized Rashba spin–orbit coupling produced by the gauge field. As shown in [7], a rashbon is the bound state of two fermions at infinite scattering length (resonance) in the presence of the non-Abelian gauge field. The crossover from the BCS state to the 'rashbon BEC' (RBEC) state induced by the gauge field at a fixed scattering length is to be contrasted with the traditional BCS–BEC crossover [8–11] by tuning the scattering length [12–14], but with no gauge field. Gong *et al* [15] have investigated the crossover including the effects of a Zeeman field along with a non-Abelian gauge field. The BCS–BEC crossover and certain properties of rashbons in the extreme oblate (EO) gauge field (explained later) have been investigated in [16] and [17]. The role of population imbalance has also been investigated [18].

It was shown in [7] that the Fermi surface of the noninteracting system (with $a_s = 0$) in the presence of the non-Abelian gauge field undergoes a change in topology at a critical gauge coupling strength λ_T (of order k_F). For weak attractions ($-1/k_F a_s \gg 1$), the regime of the gauge coupling strengths, where the crossover from the BCS state to the RBEC state takes place, coincides with the regime where the bare Fermi surface undergoes the topology change. The properties of the superfluid state (such as the transition temperature) for $\lambda \gtrsim \lambda_T$ were argued to be determined primarily by the properties of the constituent anisotropic rashbons. It is therefore necessary and fruitful to conduct a detailed study of the properties of rashbons and their dispersion, and this is the aim of this paper.

In this paper, we study the properties of rashbons and their dependence on the nature of the non-Abelian gauge field, i.e. we obtain the properties of rashbons for the most interesting GFCs. This study entails a study of the anisotropic rashbon dispersion, i.e. the determination of its energy as a function of its momentum by the study of the two-body problem in a non-Abelian gauge field with a resonant scattering length ($1/\lambda a_s = 0$). In addition to the determination of the properties of rashbons, we report here a new qualitative result. It is shown that *when the momentum of a rashbon exceeds a critical value which is of the order of the gauge coupling strength, it ceases to exist*. Stated otherwise, when the center-of-mass momentum of the two fermions that make up the bound pair exceeds a value of the order of the gauge coupling strength, the bound state disappears. To uncover the physics behind this result, the two-fermion problem in a gauge field is investigated in detail for a range of scattering lengths and center-of-mass momenta. The study reveals a hitherto unknown feature of the non-Abelian gauge fields: while the non-Abelian gauge field acts as an attractive interaction amplifier for fermions with center-of-mass momenta q much smaller than the gauge field strength ($q \ll \lambda$), *the gauge field suppresses the formation of bound states of fermions with large center-of-mass momenta ($q \gtrsim \lambda$)*. In fact, it is demonstrated here that when $q \gtrsim \lambda$, a *positive* scattering length (very strong attraction) is necessary to induce a bound state of the two fermions, quite contrary to $q \ll \lambda$ where a bound state exists (essentially) for any scattering length.

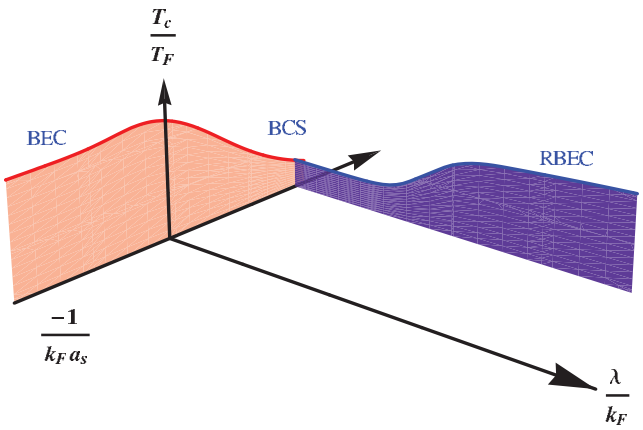

Figure 1. BCS–RBEC crossover induced by a non-Abelian gauge field. Here, a_s is the s-wave scattering length, k_F is the Fermi momentum determined by the density, T_F is the Fermi temperature ($= k_F^2/2$), T is the temperature and λ is the strength of the gauge coupling. The solid red line represents the transition temperature of the superfluid phase (shaded in light red) obtained in [19] using the Noziéres–Schmitt–Rink theory [20]. The solid blue curve is based on the estimate presented in this work. Remarkably, the T_c of the condensate obtained for $\lambda \gtrsim k_F$ is *independent of the scattering length* a_s. The figure reveals the qualitative features of the full 'phase diagram' in the T–a_s–λ space. (Figure courtesy: Sudeep Kumar Ghosh.)

The results we report here have two significant outcomes. (i) A full qualitative picture of the BCS–BEC crossover scenario in the presence of a non-Abelian gauge field is obtained (see figure 1) based on the results reported here. Most notably, it is shown that the transition temperatures of a system of fermions with a very weak attraction can be enhanced to the order of the Fermi temperature (determined by the density) by the application of a non-Abelian gauge field. (ii) Our two-body results at large center-of-mass momenta suggest that the normal state of the fermion system in a non-Abelian gauge field will be a 'dynamic mixture' of rashbons and interacting helical fermions. These could therefore show many novel features such as pronounced pseudogap characteristics (see [21] and references therein).

Section 2 contains the preliminaries including the formulation of the problem. Section 3 reports on the properties of rashbons, and this is followed by section 4, which discusses the bound state of two fermions for arbitrary center-of-mass momentum and scattering length for specific high-symmetry gauge fields. The importance of the results obtained is discussed in section 5, and the paper concludes with a summary in section 6.

2. Preliminaries

The Hamiltonian of the fermions moving in a uniform non-Abelian gauge field that leads to a generalized Rashba spin–orbit interaction is[1]

$$\mathcal{H}_R = \int d^3\boldsymbol{r}\, \Psi^\dagger(\boldsymbol{r}) \left(\frac{\boldsymbol{p}^2}{2}\mathbf{1} - \boldsymbol{p}_\lambda \cdot \boldsymbol{\tau} \right) \Psi(\boldsymbol{r}), \tag{1}$$

[1] A more detailed classification of the non-Abelian gauge fields can be found in [6, 7].

where $\Psi(\boldsymbol{r}) = \{\psi_\sigma(\boldsymbol{r})\}$, $\sigma = \uparrow, \downarrow$ are fermion operators, $\boldsymbol{p}$ is the momentum, $\mathbf{1}$ is the SU(2) identity, τ^μ ($\mu = x, y, z$) are Pauli matrices, and $\boldsymbol{p}_\lambda = \sum_i p_i \lambda_i \boldsymbol{e}_i$, $\boldsymbol{e}_i$'s are the unit vectors in the ith direction, $i = x, y, z$. The vector $\boldsymbol{\lambda} = \lambda\hat{\boldsymbol{\lambda}} = \sum_i \lambda_i \boldsymbol{e}_i$ describes a GFC space; here, $\lambda = |\boldsymbol{\lambda}|$ refers to the gauge coupling strength. Throughout, we have set the mass of the fermions (m_F), the Planck constant ($\hbar$) and the Boltzmann constant (k_B) to unity.

In this paper, we specialize to $\boldsymbol{\lambda} = (\lambda_l, \lambda_l, \lambda_r)$ as this contains all the experimentally interesting high-symmetry GFCs. Moreover, it is shown in [6, 7] that this set of gauge fields captures all the qualitative physics of the full GFC space. Specific high-symmetry GFCs are obtained for particular values of λ_r and λ_l: $\lambda_r = 0$ corresponds to EO GFC; $\lambda_r = \lambda_l$ corresponds to spherical (S) GFC; and $\lambda_l = 0$ corresponds to extreme prolate (EP) GFC.

The interaction between the fermions is described by a contact attraction in the singlet channel

$$\mathcal{H}_\upsilon = \upsilon \int \mathrm{d}^3\boldsymbol{r}\, \psi_\uparrow^\dagger(\boldsymbol{r})\psi_\downarrow^\dagger(\boldsymbol{r})\psi_\downarrow(\boldsymbol{r})\psi_\uparrow(\boldsymbol{r}). \tag{2}$$

Ultraviolet regularization [22] of the theory described by $\mathcal{H} = \mathcal{H}_\mathrm{R} + \mathcal{H}_\upsilon$ is achieved by exchanging the bare interaction υ for the scattering length a_s via $\frac{1}{\upsilon} + \Lambda = \frac{1}{4\pi a_\mathrm{s}}$, where Λ is the ultraviolet momentum cutoff. Note that a_s is the s-wave scattering length in free vacuum, i.e. when the gauge field is absent ($\lambda = 0$).

The one-particle states of $\mathcal{H}_\mathrm{R}$ are described by the quantum numbers of momentum $\boldsymbol{k}$ and helicity α (which assumes values $\pm$): $|\boldsymbol{k}\alpha\rangle = |\boldsymbol{k}\rangle \otimes |\alpha\hat{\boldsymbol{k}}_\lambda\rangle$. The one-particle dispersion is $\varepsilon_{\boldsymbol{k}\alpha} = \frac{k^2}{2} - \alpha|\boldsymbol{k}_\lambda|$, where $\boldsymbol{k}_\lambda$ is defined in an analogous manner to $\boldsymbol{p}_\lambda$, and $|\alpha\hat{\boldsymbol{k}}_\lambda\rangle$ is the spin-coherent state in the direction $\alpha\hat{\boldsymbol{k}}_\lambda$. The two-particle states of $\mathcal{H}$ can be described using the basis states $|\boldsymbol{q}\boldsymbol{k}\alpha\beta\rangle = |(\frac{\boldsymbol{q}}{2} + \boldsymbol{k})\alpha\rangle \otimes |(\frac{\boldsymbol{q}}{2} - \boldsymbol{k})\beta\rangle$, where $\boldsymbol{q} = \boldsymbol{k}_1 + \boldsymbol{k}_2$ is the center-of-mass momentum and $\boldsymbol{k} = (\boldsymbol{k}_1 - \boldsymbol{k}_2)/2$ is the relative momentum of two particles with momenta $\boldsymbol{k}_1$ and $\boldsymbol{k}_2$. Note that $\boldsymbol{q}$ is a good quantum number for the full Hamiltonian ($\mathcal{H}$). The noninteracting two-particle dispersion is $E^{\mathrm{free}}_{\boldsymbol{q}\boldsymbol{k}\alpha\beta} = \varepsilon_{(\frac{\boldsymbol{q}}{2}+\boldsymbol{k})\alpha} + \varepsilon_{(\frac{\boldsymbol{q}}{2}-\boldsymbol{k})\beta}$. In the presence of interactions, bound states emerge as isolated poles of the T-matrix, and are roots of the equation

$$\frac{1}{4\pi a_\mathrm{s}} = \frac{1}{V}\sum_{\boldsymbol{k}\alpha\beta}\left(\frac{|A^{\boldsymbol{q}}_{\alpha\beta}(\boldsymbol{k})|^2}{E(\boldsymbol{q}) - E^{\mathrm{free}}_{\boldsymbol{q}\boldsymbol{k}\alpha\beta}} + \frac{1}{4k^2}\right), \tag{3}$$

where $A^{\boldsymbol{q}}_{\alpha\beta}(\boldsymbol{k})$ is the singlet amplitude in $|\boldsymbol{q}\boldsymbol{k}\alpha\beta\rangle$, V is the volume and $E(\boldsymbol{q}) = E_\mathrm{th}(\boldsymbol{q}) - E_\mathrm{b}(\boldsymbol{q})$ is the energy of the bound state. Here $E_\mathrm{th}(\boldsymbol{q})$ is the scattering threshold and $E_\mathrm{b}(\boldsymbol{q})$ is the binding energy, both of which depend on $\boldsymbol{q}$ as indicated.

In the absence of the gauge field ($\lambda = 0$), the bound state exists only for $a_\mathrm{s} > 0$ and $E_\mathrm{b}(\boldsymbol{q}) = -1/a_\mathrm{s}^2$ is independent of $\boldsymbol{q}$. The threshold is $E_\mathrm{th}(\boldsymbol{q}) = q^2/4$. Physically, this corresponds to the fact that a critical attraction is necessary in free vacuum ($\lambda = 0$) for the formation of the two-body bound state. As shown in [6], the state of affairs changes drastically in the presence of a non-Abelian gauge field. For $\boldsymbol{q} = \mathbf{0}$, the presence of the gauge field always reduces the critical attraction to form the bound state and in particular, for special high-symmetry GFCs (e.g. $\boldsymbol{\lambda} = (\lambda_l, \lambda_l, \lambda_r)$ with $\lambda_r \leqslant \lambda_l$) the two-body bound state forms for any scattering length.

3. Properties of rashbons

The bound state that emerges in the presence of the gauge field when the scattering length is set to the resonant value $1/a_\mathrm{s} = 0$ is the rashbon. As argued above, the binding energy of the

rashbon state for all the GFCs considered here (except for the EP GFC) is positive. The energy of the rashbon state $E_{\rm R}(\boldsymbol{q}=\boldsymbol{0})$ determines the chemical potential of the RBEC. Other properties of the RBEC are determined by the rashbon dispersion $E_{\rm R}(\boldsymbol{q})$, and in particular the transition temperature will be determined by the mass of the rashbons.

The curvature of the rashbon dispersion $E_{\rm R}(\boldsymbol{q})$ at $\boldsymbol{q}=\boldsymbol{0}$ defines the effective low-energy inverse mass of rashbons. The dispersion is, in general, anisotropic and the inverse mass is, in general, a tensor. However, due to their symmetry, for the GFCs considered in this paper ($\boldsymbol{\lambda}$ of the form $(\lambda_l, \lambda_l, \lambda_r)$), $E_{\rm R}(\boldsymbol{q}) = E_{\rm R}(q_l, q_r)$, where q_l is the component of $\boldsymbol{q}$ on the x–y-plane, and q_r is the component along $\boldsymbol{e}_z$. Thus, the inverse mass tensor is completely specified by its principal elements—the in-plane inverse mass (m_l^{-1}) and the 'perpendicular' inverse mass, m_r^{-1}.

$$m_l^{-1} = \left.\frac{\partial^2 E_{\rm R}(q_l, q_r)}{\partial q_l^2}\right|_{\boldsymbol{q}=\boldsymbol{0}}, \quad m_r^{-1} = \left.\frac{\partial^2 E_{\rm R}(q_l, q_r)}{\partial q_r^2}\right|_{\boldsymbol{q}=\boldsymbol{0}}. \tag{4}$$

With some analysis, we obtain that

$$m_l^{-1} = \frac{2\sum_{\boldsymbol{k}\alpha\beta} \frac{\left.\frac{\partial^2 |A^{\boldsymbol{q}}_{\alpha\beta}(\boldsymbol{k})|^2}{\partial q_l^2}\right|_{\boldsymbol{q}=\boldsymbol{0}}}{\left(E_{\rm R}(\boldsymbol{0}) - E^{\rm free}_{\boldsymbol{0}\boldsymbol{k}\alpha\beta}\right)^2} + \sum_{\boldsymbol{k}\alpha} \frac{\left.\frac{\partial^2 E^{\rm free}_{\boldsymbol{q}\boldsymbol{k}\alpha\alpha}}{\partial q_l^2}\right|_{\boldsymbol{q}=\boldsymbol{0}}}{\left(E_{\rm R}(\boldsymbol{0}) - E^{\rm free}_{\boldsymbol{0}\boldsymbol{k}\alpha\alpha}\right)^2}}{\sum_{\boldsymbol{k}\alpha} \frac{1}{\left(E_{\rm R}(\boldsymbol{0}) - E^{\rm free}_{\boldsymbol{0}\boldsymbol{k}\alpha\alpha}\right)^2}} \tag{5}$$

and a similar expression (not shown) for m_r^{-1}. In the absence of the gauge field, the first term in the numerator vanishes because of equal and opposite contributions from like and unlike helicities and recovers $m_l = m_r = 2$. An effective mass $m_{\rm ef}$ defined as

$$m_{\rm ef} = \sqrt[3]{(m_r m_l^2)} \tag{6}$$

is useful for the discussions that follow.

In addition to the anisotropy in their orbital motion, rashbons are intrinsically anisotropic particles. Their pair-wave function has both a singlet and a triplet component; the weight of the pair-wave function in the triplet sector $\eta_{\rm t}$ is the triplet content. The triplet component is time reversal symmetric, but does not have the spin rotational symmetry—it is therefore a spin nematic. Keeping this interesting aspect in mind, we shall also investigate and report the triplet content of rashbons and its dependence on the gauge field.

Before presenting the results we make some general observations. The threshold energy ($E_{\rm th}$) becomes increasingly flat as a function of $\boldsymbol{q}$ in the small $\boldsymbol{q}/\lambda$ regime as one approaches the spherical gauge field in the GFC space. In fact, for the S GFC, it is exactly constant in the small $\boldsymbol{q}/\lambda$ regime (see figure 3). The mass is therefore determined entirely by the variation of the binding energy with $\boldsymbol{q}$ (this may be contrasted in the free vacuum case discussed before). It is reasonable therefore to expect that the effective mass of rashbons is always greater than twice the bare fermion mass and for it to be the largest for the S GFC.

Figure 2(a) shows the in-plane, perpendicular and effective masses for different GFCs. Rashbons emerging from S GFCs have the highest $m_{\rm ef}$ and that from EP GFCs have the least. It is interesting to note that apart from the S GFC, there is yet another GFC ($\lambda_r \approx 0.65\lambda$—see figure 2(a)), where the low-energy dispersion is isotropic, i.e. the rashbon has a scalar mass. The triplet content is shown in figure 2(b) for different GFCs. $\eta_{\rm t}$ is minimum (1/4) for S GFC and maximum (1/2) for EP GFC.

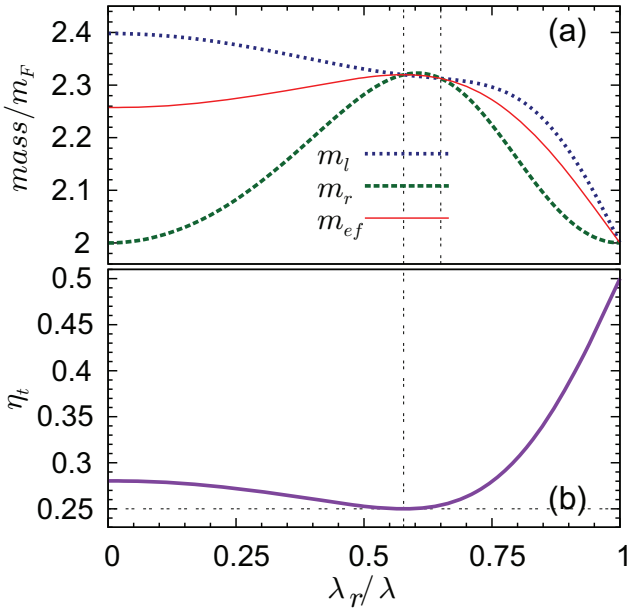

Figure 2. Rashbon properties for different GFCs. (a) The in-plane, perpendicular and effective masses. (b) The triplet content of rashbons.

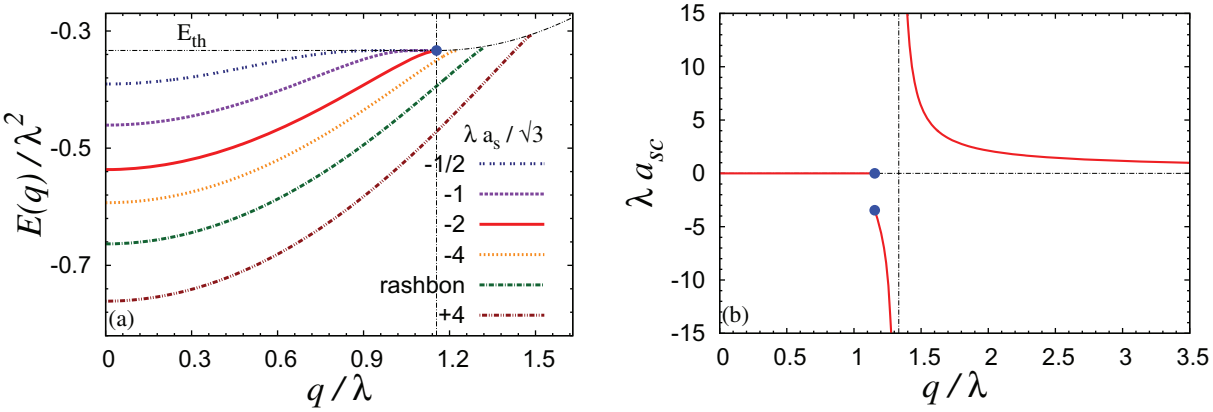

Figure 3. (a) The boson dispersion for various scattering lengths in S GFC. Note that for any given scattering length, the bound state disappears after some critical momentum. (b) The critical scattering length (a_{sc}) as a function of momentum. a_{sc} goes as $1/\sqrt{q}$ in the large q/λ limit.

A detailed study of rashbon dispersion as a function of its momentum $\boldsymbol{q}$ (center-of-mass momentum of the fermions that make up the rashbon) revealed a hitherto unreported and rather unexpected feature. The full rashbon dispersion as a function of $\boldsymbol{q}$ for the S GFC is shown in figure 3. The rashbon energy increases with increasing q and eventually for $q/\lambda \gtrsim 1.3$, there is no two-body bound state! This curious result motivated us to perform a more detailed investigation of the dispersion of the bound fermions (bosons) at arbitrary scattering lengths (away from resonance which corresponds to rashbons), in order to uncover the physics behind this phenomenon. This study, conducted for specific high-symmetry GFCs, is presented in the next section.

4. Dispersion of bosons at arbitrary scattering lengths for specific gauge field configurations (GFCs)

In this section, we investigate the dispersion of the bosonic bound state of two fermions at arbitrary scattering lengths. The results of the boson dispersion obtained by solving equation (3) will be presented for the S, EO and EP GFCs.

4.1. Spherical GFC

S GFC corresponds to $\lambda_r = \lambda_l$ and hence produces an isotropic boson dispersion as discussed before. The boson dispersion depends only on $q = |\boldsymbol{q}|$. Solving equation (3), the boson dispersion obtained for various scattering lengths is as shown in figure 3(a). The key features of this spectrum are the following. For *any attraction, however large* (small and positive scattering length), there exists a critical center-of-mass momentum q_c such that when $q > q_c$ the bound state ceases to exist.

This is best understood by fixing our attention on a particular momentum q. When the momentum is 'small', there is a bound state for *any attraction*. This is in fact the case for all $q < q_o$, where $q_o = 2\frac{\lambda}{\sqrt{3}}$. For $q > q_o$, a critical attraction described by a nonzero scattering length a_{sc} is necessary for the formation of a bound state. For $q = q_o^+$, the critical scattering length is $a_{sc} = -\frac{2\sqrt{3}}{\lambda}$. With increasing q, a stronger attractive interaction is required to produce a bound state, and when q reaches $\sim\frac{4\lambda}{3}$, a resonant attraction is necessary to produce a bound state. For $q \gtrsim \frac{4\lambda}{3}$, a very strong attractive interaction described by a small positive scattering length is necessary to produce a bound state. In fact, for $q \gg \lambda$, the critical scattering length scales as $a_{sc} \sim \sqrt{\frac{1}{\lambda q}}$. The dependence of a_{sc} on the center-of-mass momentum is shown in figure 3(b).

How do we understand these results? Here the ε_0–γ model introduced in [6] comes to our rescue. The model states that if the infrared singlet density of states $g_s(\varepsilon) \sim \varepsilon^\gamma$ for $0 \leqslant \varepsilon \leqslant \varepsilon_0$, where ε is the energy measured from the scattering threshold, then the critical scattering length is given by $\sqrt{\varepsilon_0} a_{sc} \propto \gamma\, \Theta(\gamma)/(2\gamma - 1)$, where Θ is the unit step function. Note that for $\gamma \leqslant 0$, the critical scattering length vanishes.

It is evident that there is a drastic change in the infrared density of states at $q = q_o$. In fact, this special momentum q_o is such that the threshold energy corresponds to that state where the relative momentum $\boldsymbol{k}$ between the pair of fermions vanishes. Clearly, for $q < q_o$, there are many degenerate $\boldsymbol{k}$ states that produce a nonzero density of states at the threshold. In fact, when $q = 0$, the density of states diverges as $1/\sqrt{\varepsilon}$, i.e. $\gamma = -1/2$. For $q < q_o$, there is still a finite density of states at the threshold with an effective $\gamma < 0$. Thus the critical scattering length, as given by the ϵ_0–γ model, vanishes. Let us turn our attention to what happens for $q \gg \lambda$. From equation (3) it is evident that the density of states $g_s(\varepsilon)$ has the contributions from the ++, −−, +− and −+ channels. It can be shown that in the regime $q \gg \lambda$, the ++ channel has a density of states that has $\varepsilon^{3/2}$ behavior. The +− and −+ channels have a threshold which is λq larger than the threshold of the ++ channel; the density of states of the $+-/-+$ channels goes as $\sqrt{\varepsilon}$ from this higher threshold. These arguments provide an estimate of $\varepsilon_0 \approx q\lambda$. The result on the critical scattering length is then $a_{sc} \sim \frac{1}{\sqrt{q}}$, precisely as obtained from the full numerical solution shown in figure 3(b).

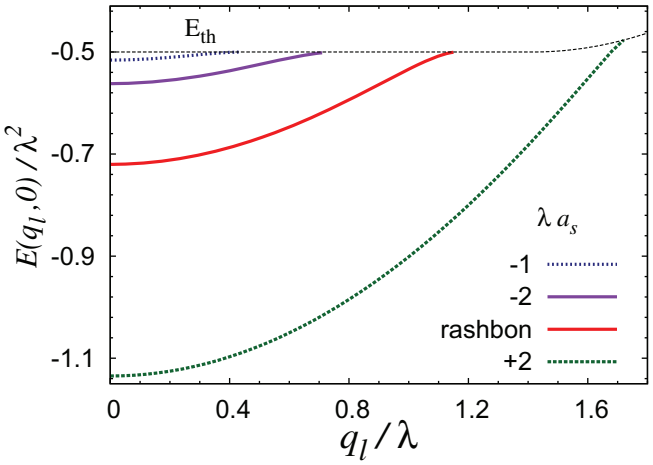

Figure 4. The boson dispersion for various scattering lengths in EO GFC. Just as in S GFC (see figure 3), for any given scattering length, the bound state disappears after some critical q_l. In the rashbon case this critical q_l is $\approx 1.15\lambda$.

As a byproduct of the analysis of the boson dispersion, we are able to obtain an analytical expression for the mass of bosons (which is isotropic in this case)

$$\frac{m_{\mathrm{B}}}{m_{\mathrm{F}}} = \frac{6}{7 + \frac{2\lambda^2}{E(\mathbf{0})} - 4\left(1 + \frac{\lambda^2}{3E(\mathbf{0})}\right)^{3/2}}, \tag{7}$$

where

$$E(\mathbf{0}) = -\frac{\lambda^2}{3} - \frac{1}{4}\left(\frac{1}{a_{\mathrm{s}}} + \sqrt{\frac{1}{a_{\mathrm{s}}^2} + \frac{4\lambda^2}{3}}\right)^2. \tag{8}$$

At a given λ, as expected, the mass for a small positive scattering length $a_{\mathrm{s}} > 0$ is twice the fermion mass. The mass at resonance is the rashbon mass, which is equal to $= \frac{3}{7}(4+\sqrt{2})m_{\mathrm{F}} \approx 2.32m_{\mathrm{F}}$. Interestingly, the value of $m_{\mathrm{B}}/m_{\mathrm{F}}$ in the small negative scattering length limit is (integer) 6.

4.2. Extreme oblate GFC

EO GFC corresponds to $\lambda_r = 0$ with $\lambda_l = \frac{\lambda}{\sqrt{2}}$. It can be easily shown that for this GFC, $E(q_l, q_r) = E(q_l, 0) + \frac{q_r^2}{4}$. Thus, the two-body dispersion as a function of q_l provides all the nontrivial features of the two-body problem arising from this gauge field.

Figure 4 shows the boson dispersion for various scattering lengths. Remarkably, we find that the dispersion has very similar features as found for the S GFC, i.e. for any given scattering length there is a q_{c} such that for $q_l > q_{\mathrm{c}}$, the two-body bound state ceases to exist. Clearly, this is a generic feature of the boson (bound fermion-pair) dispersion in a gauge field.

For this GFC, m_r is just twice the fermion mass. The in-plane mass (m_l) extracted from the two-body dispersion is shown in figure 5. m_l for small positive scattering length is again twice the fermion mass. The resonance value which corresponds to rashbon is $m_l \simeq 2.4m_{\mathrm{F}}$. This result agrees with [16, 17]. It is again interesting to note that the value of m_l/m_{F} in the small negative scattering length limit is (integer) 4.

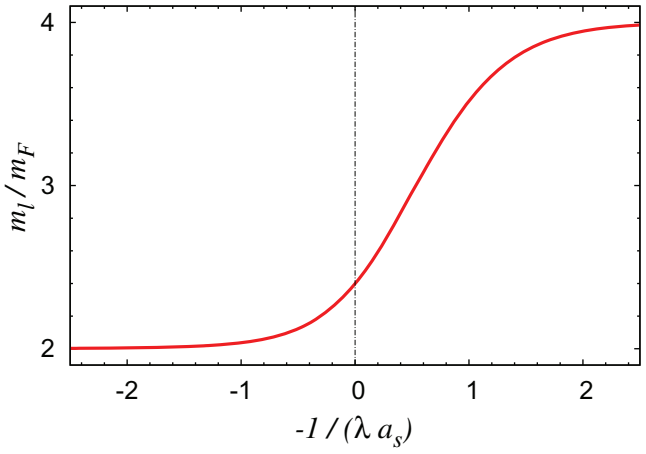

Figure 5. In-plane mass of tightly bound fermion pairs in the RBEC side in the presence of an EO GFC.

4.3. Discussion

The analysis of the dispersion of the boson (bound state of two fermions obtained in a gauge field) reveals that the boson ceases to exist when its momentum exceeds a critical value. For the case of rashbons (bosons obtained at resonant scattering length), the critical momentum is of the order of the strength of the gauge field.

The analysis presented here shows that this is again because of the influence of the gauge field in altering the infrared density of states. When the momentum is smaller than the magnitude of the gauge coupling, the gauge field works to *enhance* the infrared singlet density of states. On the other hand, for large momenta, the gauge field has the opposite effect, i.e. it *depletes* the infrared singlet density of states.

4.4. Extreme prolate GFC

For the sake of completeness, we now discuss the two-body problem in EP GFC, which corresponds to $\lambda_l = 0$ or equivalently $\lambda_r = \lambda$. In this GFC, $E(\boldsymbol{q}) = E(\boldsymbol{0}) + \frac{q^2}{4}$, and the mass is isotropic and is equal to twice the fermion mass, i.e. $m_r = m_l = 2m_{\mathrm{F}}$.

The threshold energy (which corresponds to the noninteracting two-body ground state) varies with the center-of-mass momentum as

$$E_{\mathrm{th}}(\boldsymbol{q}) = \begin{cases} \frac{q^2}{4} - \lambda^2 & \text{if } |q_r| < \lambda, \\ \frac{q^2}{4} - \lambda|q_r| & \text{if } |q_r| \geqslant \lambda. \end{cases} \tag{9}$$

This is shown in figure 6 (solid red curve). The singlet density of states goes as $\sqrt{\varepsilon}$ starting from $\frac{q^2}{4} - \lambda^2$. We refer to this threshold as the singlet threshold (shown by the dashed blue curve). This is exactly the density of states in the absence of the gauge field starting from $\frac{q^2}{4}$. Thus, the bound state exists only for $a_{\mathrm{s}} > 0$ and the binding energy is independent of $\boldsymbol{q}$ and is given by $E_{\mathrm{b}} = \frac{1}{a_{\mathrm{s}}^2}$.

The noninteracting two-particle states with energies lying between the total and the singlet thresholds (represented by the yellow shade in figure 6) are *pure* triplet states. The interaction,

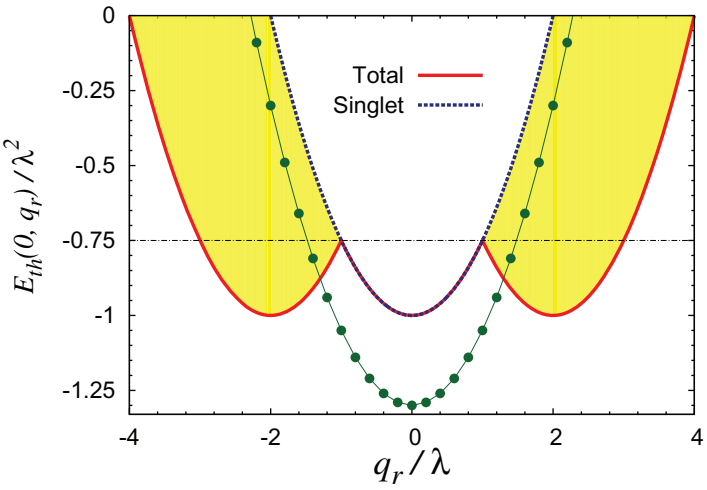

Figure 6. The singlet (dashed blue curve) and the total (solid red curve) threshold energies as a function of q_r of two fermions in EP GFC. The pure triplet states are shown in yellow shading. It can be seen that the bound states (green dots) formed by the attraction in the singlet channel can be higher in energy than the free two-fermion triplet states.

which is in the singlet channel, produces bound states whose energies are below the singlet threshold by $E_b = \frac{1}{a_s^2}$ (represented by green dots in figure 6). Note that there can be unbound triplet states lower in energy compared to these bound singlet states. This feature can also be seen in GFCs with $\lambda_r > \lambda_l$.

5. Significance of the results

The above results allow us to infer many key aspects of the physics of interacting fermions in the presence of a non-Abelian gauge field.

First, these results allow us to estimate the transition temperature. For large gauge couplings, the transition temperature as noted above will be determined by the mass of the rashbons. We have argued (and demonstrated) that the mass of the rashbons is always greater than twice the fermion mass. Thus the transition temperature of RBEC will always be less than that of the usual BEC of bound pairs of fermions obtained in the absence of the gauge field by tuning the scattering length to small positive values.

However, there is something remarkable that a synthetic non-Abelian gauge field can achieve. Consider a system with a weak attraction (small negative scattering length). In the absence of the gauge field, the transition temperature in the BCS superfluid state is exponentially small in the scattering length. Interestingly, the transition temperature can be brought to the order of the Fermi temperature by increasing the magnitude of the gauge field strength (keeping the weak attraction, small negative scattering length, fixed).

While T_c in the BCS regime is determined by the pairing amplitude (Δ), in the BEC regime it is determined by the condensation temperature of the emergent bosons [20], rashbons in the present case.

The mean field estimate of the former (i.e. for small $k_F|a_s|$, $a_s < 0$ and small λ/k_F) is obtained by simultaneously solving $-1/(4\pi a_s) = \frac{1}{2V}\sum_{k\alpha}\left(\frac{\tanh\frac{\xi_{k\alpha}}{2T_c}}{2\xi_{k\alpha}} - \frac{1}{k^2}\right)$ and the number equation $\rho = \frac{1}{V}\sum_{k\alpha} 1/\left(\exp\left(\frac{\xi_{k\alpha}}{T_c}\right)+1\right)$, where $\xi_{k\alpha} = \varepsilon_{k\alpha} - \mu$. In this limit, the chemical potential at T_c is almost equal to that of the noninteracting one at zero temperature, i.e. $\mu(T_c, a_s, \lambda) \approx \mu(0, 0^-, \lambda)$, and $\Delta_{(T=0)}/T_c \approx \pi/e^{\gamma}$ where [7] $\Delta_{(T=0)}$ is the pairing amplitude at zero temperature and γ is Euler's constant (≈ 0.577).

The T_c on the RBEC side can be extracted from the effective mass (m_{ef}) as the condensation temperature of the bosonic pairs:

$$\frac{T_c}{T_F} = \left(\frac{16}{9\pi(\zeta(3/2))^2}\right)^{1/3}\frac{1}{m_{ef}} \quad \text{(RBEC)}, \tag{10}$$

where we recall that $m_{ef} = (m_r m_l^2)^{1/3}$. Using the information of mass given earlier (equation (7) for S GFC and figure 5 for EO GFC) one can obtain T_c in this regime as a function of λa_s in S and EO GFCs. In particular, rashbon T_c in the S case is $\approx 0.188T_F$ and in the EO case it is $\approx 0.193T_F$. The rashbon T_c can be obtained for various GFCs, using m_{ef} shown in figure 2(a). Since, among all GFCs, the rashbon mass corresponding to S GFC is the largest, it also corresponds to the condensate with the smallest T_c.

The results obtained in both BCS and RBEC limits for $k_F a_s = -1/4$ in S and EO GFCs are shown in figure 7. We can see, as advertised, that T_c increases by two orders of magnitude with increasing gauge coupling strength λ. These considerations, along with the fact that T_c of the condensate when $\lambda \gg k_F$ is the same for all a_s, also allow us to infer an overall qualitative 'phase diagram' in the T–a_s–λ space as shown in figure 1.

What is the nature of the system above T_c? The parameter space shown in figure 1 contains a regime where the normal state can be quite interesting. Consider, for example, $\lambda \approx 1.5k_F$. The ground state will be 'very bosonic', i.e. a condensate of rashbons in the zero-momentum state. On heating the system above the transition temperature $\lesssim T_F$, the system becomes normal. At these temperatures, there is a thermal breakup of rashbons. On top of this, rashbons that are excited to higher momenta states break up into the constituent fermions since there is no bound state at higher momenta. There should, therefore, be a temperature range where the system is a dynamical mixture of uncondensed rashbons and high-energy helical fermions—a state that should show many novel features such as, among other things, a pseudogap. It is interesting to note that the effects of the non-Abelian gauge field should also be observable at higher temperatures than T_c.

These results also suggest important consequences for the structure of topological defects in the superfluids induced by the gauge field. In particular, the fact that the bosonic pairs will cease to exist above a critical center-of-mass momentum suggests that pair breaking effects will be quite significant at the core of the vortices of such superfluids.

6. Summary

The new results of this paper are as follows:

1. A systematic enumeration of the properties of rashbons, including closed-form analytical formulae, for various GFCs.

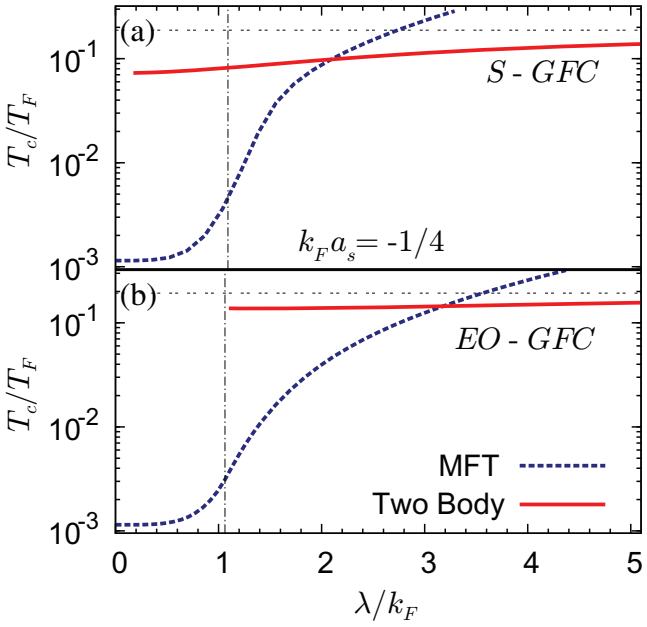

Figure 7. Estimate of the transition temperature in S and EO GFCs as a function of the gauge coupling strength which takes the regular BCS state to an RBEC. T_c in the small λ/k_F limit is obtained from mean field theory (analytical approximation is shown in the text). T_c in the large λ/k_F limit is obtained from the condensation temperature of the tightly bound pairs of fermions (the analytical form of the S GFC can be obtained from equations (7) and (10)). The horizontal dashed line corresponds to rashbon T_c. The vertical line indicates the gauge coupling corresponding to the Fermi surface topology transition [7].

2. A detailed study of the rashbon (boson) dispersion, which results in a new qualitative observation. Although a zero center-of-mass momentum bound state exists for any scattering length for many GFCs, the bound state vanishes when the center-of-mass momentum exceeds a critical value. Thus, although the gauge field acts to promote bound state formation for small momenta, it acts oppositely, i.e. inhibits bound state formation for large momenta. We provide a detailed explanation of the physics behind the phenomenon.

These results allow us to make two important inferences:

1. For a fixed weak attractive interaction, the exponentially small transition temperature of a BCS superfluid can be enhanced by orders of magnitude to the order of the Fermi temperature of the system by increasing the magnitude of the gauge coupling.
2. There is a regime of T–a_s–λ parameter space where the normal phase of the system will have novel features.

It is evident from these conclusions that systems with spin–orbit coupling generated via synthetic non-Abelian gauge fields provide a platform for exploring new states of interacting fermions. Furthermore, these systems also provide opportunities for the realisation of exotic

objects such as magnetic monopoles [23]. We hope that this will stimulate further experimental and theoretical studies on this topic.

Acknowledgments

JV acknowledges support from CSIR, India via a JRF grant. VBS is grateful to DST, India (Ramanujan grant) and DAE, India (SRC grant) for generous support. We are grateful to Sudeep Kumar Ghosh for providing us with figure 1.

References

[1] Lin Y-J, Compton R L, Perry A R, Phillips W D, Porto J V and Spielman I B 2009 *Phys. Rev. Lett.* **102** 130401
[2] Lin Y-J, Compton R L, Jimenez-Garcia K, Porto J V and Spielman I B 2009 *Nature* **462** 628
[3] Lin Y-J, Jimenez-Garcia K and Spielman I B 2011 *Nature* **471** 83
[4] Ho T-L and Zhang S 2010 arXiv:1007.0650
[5] Wang C, Gao C, Jian C-M and Zhai H 2010 *Phys. Rev. Lett.* **105** 160403
[6] Vyasanakere J P and Shenoy V B 2011 *Phys. Rev.* B **83** 094515
[7] Vyasanakere J P, Zhang S and Shenoy V B 2011 *Phys. Rev.* B **84** 014512
[8] Eagles D M 1969 *Phys. Rev.* **186** 456
[9] Leggett A J 1980 *Modern Trendsin the Theory of Condensed Matter* ed A Pekalski and R Przystawa (Berlin: Springer) pp 13–27
[10] Randeria M 1995 *Bose–Einstein Condensation* ed A Griffin, D Snoke and S Stringari (Cambridge: Cambridge University Press) chapter 15
[11] Leggett A J 2006 *Quantum Liquids: Bose Condensation and Cooper Pairing in Condensed-Matter Systems* (Oxford: Oxford University Press)
[12] Regal C A, Greiner M and Jin D S 2004 *Phys. Rev. Lett.* **92** 040403
[13] Ketterle W and Zwierlein M W 2008 arXiv:0801.2500
[14] Giorgini S, Pitaevskii L P and Stringari S 2008 *Rev. Mod. Phys.* **80** 1215
[15] Gong M, Tewari S and Zhang C 2011 arXiv:1105.1796
[16] Hu H, Jiang L, Liu X-J and Pu H 2011 arXiv:1105.2488
[17] Yu Z-Q and Zhai H 2011 arXiv:1105.2250
[18] Iskin M and Subaısnfi A L 2011 *Phys. Rev. Lett.* **107** 050402
[19] Sá de Melo C A R, Randeria M and Engelbrecht J R 1993 *Phys. Rev. Lett.* **71** 3202
[20] Noziéres P and Schmitt-Rink S 1985 *J. Low Temp. Phys.* **59** 195
[21] Mueller E J 2011 *Phys. Rev.* A **83** 053623
[22] Braaten E, Kusunoki M and Zhang D 2008 *Ann. Phys.* **323** 1770
[23] Ghosh S K, Vyasankere J P and Shenoy V B 2011 *Phys. Rev.* A **84** 053629